# Numerical Study of Fish Scales Structure on the Flow Loss Reduction in Compressor Cascade

Jin-Long Shen, Ho-Chun Yang and Szu-I Yeh *

Department of Aeronautics and Astronautics, National Cheng Kung University, Taiwan

* siyeh@mail.ncku.edu.tw

**Abstract**

As the demand for high-performance compressors grows, traditional designs face challenges in efficiency and stability. This study uses OpenFOAM simulations to explore bionic fish-scale structures, analyzing parameters like scale heights (0.4 to 0.8 mm) and spacings (2, 3, and 6 mm) to reduce secondary flow losses and enhance stability. Results show that a scale height of 0.4 mm and spacing of 2 mm maintain a crucial recirculation zone for drag reduction and improve fluid acceleration. The fish-scale structure also reduces secondary flow losses by suppressing corner separation and mitigating vortex effects, leading to significantly lower total pressure loss compared to conventional designs.

***Keyword:*** *Compressor Cascade, Corner separation, Fish scales, Biomimetics*

## 1. Introduction

In the 15th century, Leonardo da Vinci observed bird flight patterns and conceptualized biomimetic aircraft designs, which later inspired aviation development. Biomimetics, aimed at creating efficient engineering systems by studying biological systems, has broad applications in fields like mechanical engineering, materials science, and medicine [1]. In 1991, D. M. Bushnel highlighted the role of biological materials and structures in drag reduction [2]. These structures have spurred innovations, especially in designing efficient vehicles and fluid systems. For instance, shark skin-inspired surfaces have reduced air resistance in aircraft and wind turbine blades. However, applying biomimetic designs to compressors remains challenging due to complex internal flow fields, flow separation, and the need for strong structural integrity. Improving compressor performance, stability, and noise reduction through biomimetic structures is an ongoing research focus.

In 2021, in search of better biomimetic blade designs, Zhang proposed innovative biomimetic flow control methods for blades, including surface riblet structures, leading-edge tubercles, and trailing-edge serrations, inspired by shark skin, whale fins, and owl wings. These methods have been shown to reduce drag, lower noise, and delay stall [3]. These biological structures, refined through long-term evolution, offer high efficiency and stable flow control. Mimicking such structures opens new possibilities and technical support for advanced blade designs. With the development of simulation tools, the search for efficient biomimetic compressor blade designs is emerging as a promising research direction. Liu's research on shark skin structures revealed that modifying different structural shapes can significantly reduce airflow friction losses [4]. However, this structure's effectiveness in reducing friction only occurs when aligned horizontally with the airflow direction. When positioned vertically or at large angles to the airflow, flow separation occurs, and after optimization, the structural strength of the design significantly decreases, posing a drawback for compressors with complex flow fields that require high structural integrity. Dong found that whale fins, similar to vortex generators, can significantly increase local flow velocities, reduce drag, and improve flow efficiency. By altering the placement and size of these structures, compressor blades can more effectively reduce losses [5]. Therefore, this study aims to analyze the potential of biomimetic structures in compressor blade design by leveraging unique biological configurations. In this study we utilize OpenFOAM for simulating and analyzing secondary flow losses and improving the compressor cascade flow field without compromising structural strength through mimicking the fish scale structure of grass carp.

## 2. Methodology

### 2.1 Model design

The bionic configuration adopted in this study is based on the scales of the grass carp. Specifically, the design parameters are centered around a scale height H 0.5mm and a corresponding scale spacing Lspace 3.75 mm. The study involves varying the scale height H from 0.4 mm to 0.8 mm and adjusting the scale spacing Lspace to 2, 3, and 6 mm as the primary parameters for analyzing the flow field and the working mechanism of the bionic configuration. All other parameters are proportionally scaled, with the spacing being adjusted independently to 2 mm and 6 mm at a fixed height of 0.4 mm. A schematic diagram of the bionic grass carp scale configuration is shown in Fig. 1(a), where the scale height (H) is defined as the distance from the base to the highest point at the center of the scale.

The objective of this study is to investigate a bionic compressor cascade blade. The compressor cascade blade utilized in this study is based on the NACA-65 series. The design parameters include an inlet blade angle of 45 degrees, a turning angle of 22.5 degrees, a solidity of 1.92, and an angle of attack of 15 degrees. These parameters are within the range that ensures stable operation, with the high solidity contributing to the reduction of total pressure loss. Detailed schematic diagrams of the cascade blade design and the aerodynamic parameters are provided in Fig. 1(b). In this study, the bionic fish scales are distributed on the upper surface of the blade, within the region from 0.4 to 0.8 x/c, and positioned 7 mm from the endwall. Schematic diagrams of the bionic cascade blade design are shown in Fig. 1(c).

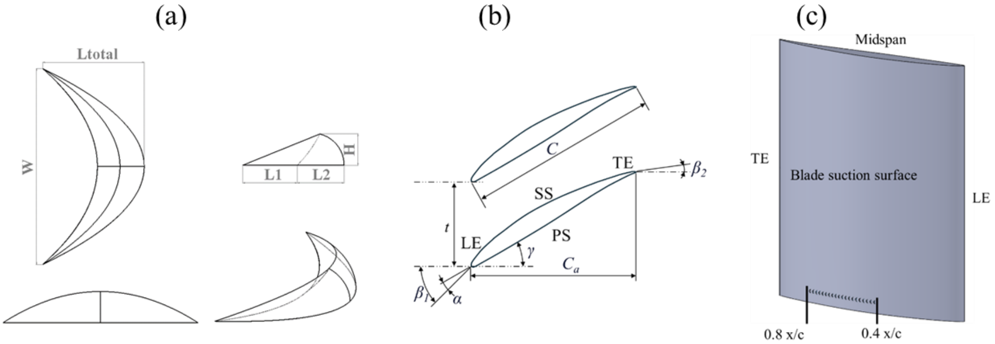


**Fig. 1 (a) Grass carp scale configuration with varying scale height (H) and spacing (Lspace). (b) NACA-65 compressor cascade blade design. (c) Bionic scale distribution on the blade surface.**

### 2.3 Simulation software and numerical methods

This study utilizes OpenFOAM for numerical simulations to investigate the flow field and interaction characteristics of the bionic grass carp scale structure on both flat-plate surfaces and cascade blades. The inlet velocity is set at 20 m/s, and the fluid is modelled as steady-state, incompressible flow using the simpleFoam solver. The flow fields around the flat-plate bionic scales and the bionic cascade blades are solved using the Reynolds-Averaged Navier-Stokes (RANS) equations. The turbulence model for the flat-plate bionic grass carp scales simulation is k-ε. For the cascade blade simulation, the SST model is selected over the k-ω and k-ε models, as it is a two-equation eddy-viscosity model that calculates for turbulent shear stress transport, allowing for more accurate prediction of flow separation.

### 2.3 Mesh setup and computational validation

In this study, the mesh was generated using Fluent Meshing and subsequently imported using the Fluent3DMeshToFoam command. The detailed design and mesh diagrams for the flat-plate bionic grass carp scales and the cascade blade computational models are illustrated in Fig. 2. The dimensions of the flat-plate bionic grass carp scale computational model are 150 mm in length (X), 8.5 mm in width (Y), and 10 mm in height (Z). To prevent interference between the flow field around the scales and the smooth surface computational domain, the height was adjusted to 10 mm. Additionally, the computational domain length was extended to 150 mm to better capture the flow phenomena and development around the bionic fish scales. To compare the bionic scale surface with a smooth surface, the bottom surface was designated as the bionic scale plane, while the top surface was set as the smooth plane. In the cascade blade computational model, periodic boundary conditions were established, and axial symmetry was assumed at the mid-plane of the blade to reduce the computational domain. The overall computational domain was meshed using unstructured tetrahedral grids. Furthermore, to more accurately simulate the flow characteristics of the boundary layer and improve orthogonality with surface features, the mesh near the wall was refined. The first layer of the mesh was set to a thickness of 1.5×10-6 m, with a linear growth rate of 1.05, ensuring that y+ ≈ 1.

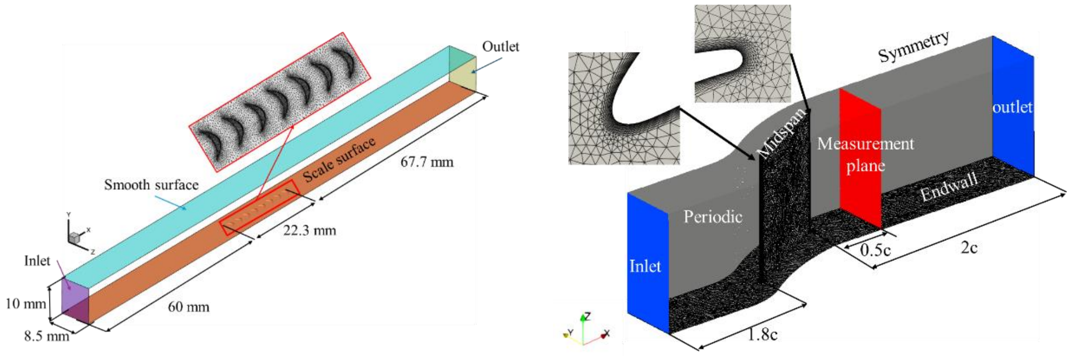


**Fig. 2 Computational model design and mesh diagram of flat-plate bionic grass carp scales and cascade blades.**

To reduce computation time and improve accuracy, mesh independence tests were conducted for both computational models, as shown in Fig. 3. For the flat-plate bionic grass carp scale model, the total mesh count of approximately7×106 resulted in a discrepancy of about 5% compared to boundary layer theory. For the traditional and bionic cascade blade models, mesh saturation was achieved at approximately $4.7\times10^6$ elements, with a further increase to $6.6\times10^6$ resulting in a difference of about 2%.

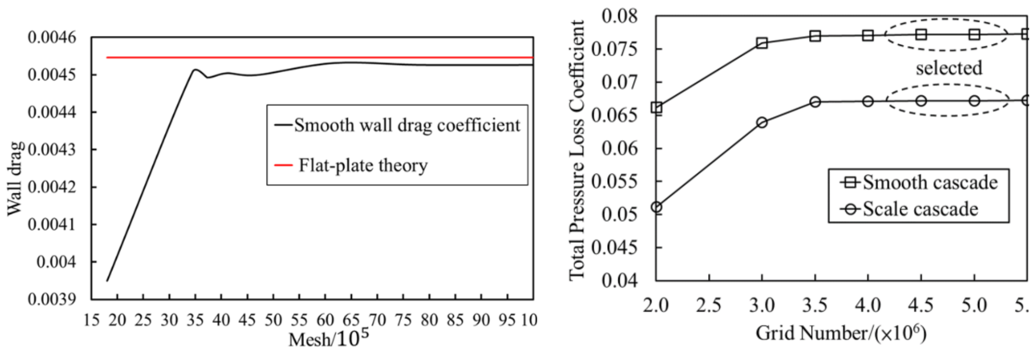


**Fig. 3 Grid independence test of flat-plate bionic grass carp scales and cascade blades**

## 3. Results and discussion

The analysis of pressure and viscous drag for different fish scale geometries, as shown in Table 2, reveals that the total drag is highest at a height of 0.8 mm and lowest at 0.4 mm. The geometric shape of the biomimetic structure mainly affects pressure drag, suggesting potential for further optimization. The viscous drag, which is equivalent to the total drag of a smooth surface, shows a 21% reduction at a 0.4 mm height, highlighting the structure's effectiveness in reducing drag. Overall, height significantly impacts total drag, while changing Lspace has minimal effect. To analyze the changes in drag caused by the bionic fish scale structure, the study will delve into the reasons behind the variations in total drag. DV represents the change in viscous drag, and DT represents the change in total drag. This analysis aims to understand the contribution of pressure drag to the overall drag variation.

As shown in Fig. 4, the low-velocity regions at the leading edge of the fish scales are recirculation zones, and similar recirculation zones are observed between the scales. These recirculation zones between the scales redirect the fluid back to the trailing edge and towards the highest point of the scales. Due to the conservation of mass, the position of the highest point on the scales is influenced by both the incoming flow and the recirculation, resulting in an acceleration of the fluid at this peak. This suggests that the presence of recirculation zones is a key factor in reducing viscous drag. The impact of recirculation zones on viscous drag is significant. Further investigation was conducted to examine the effect of changing the spacing between fish scales on the recirculation zones, as shown in Fig. 5. It is clearly observed that when the spacing is 2 mm, the recirculation zone slightly expands upward, enhancing the recirculation effect within the zone and leading to a greater reduction in viscous drag.

**Table 1 Flat-plate fish scale simulation results and resistance analysis**

| Case | $F_{smooth}$ ($N\times10^{-3}$) | Pressure drag ($N\times10^{-3}$) | Viscous drag ($N\times10^{-3}$) | Total drag ($N\times10^{-3}$) | DV (%) | DT (%) |
|---|---|---|---|---|---|---|
| H0.8 | 1.502 | 1.020 | 1.496 | 2.516 | -0.37 | 67.56 |
| H0.7 | 1.501 | 0.871 | 1.428 | 2.299 | -4.92 | 53.08 |
| H0.6 | 1.501 | 0.538 | 1.401 | 1.939 | -6.69 | 29.14 |
| H0.5 | 1.501 | 0.272 | 1.202 | 1.475 | -19.87 | -1.71 |
| H0.4 | 1.500 | 0.152 | 1.182 | 1.335 | -21.18 | -11.00 |
| L2 | 1.498 | 0.248 | 1.169 | 1.293 | -21.96 | -13.685 |
| L6 | 1.511 | 0.324 | 1.257 | 1.457 | -16.80 | -3.583 |

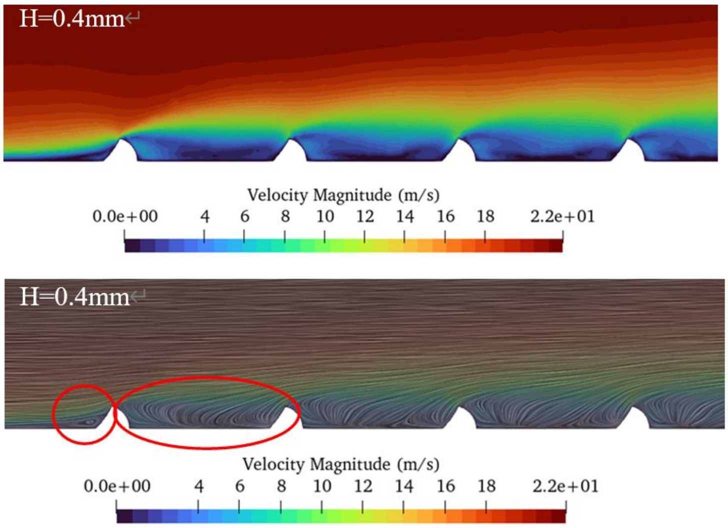


**Fig. 4 Velocity flow field at the highest point section of the fish scale with a height of 0.4 mm**

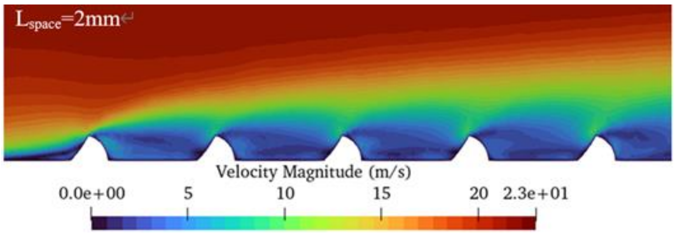


**Fig. 5 Velocity flow field at the highest point section of the fish scale with a Lspace of 2 mm**

As shown in Fig. 6, the recirculation zones in the biomimetic fish scale cascade are smaller than those in a traditional cascade. Additionally, after the formation of local low-velocity regions, the accelerated flow induced by the fish scales significantly clears these low-velocity areas within the channel. This indicates that the biomimetic fish scale cascade can inhibit the development of corner separation lines. To further understand the impact of the fish scale structure on the cascade, as shown in Fig. 7. Starting from approximately 0.6x/c, the recirculation zone at the trailing edge of the scales rises. This is due to the curvature of the blade surface and the influence of channel vortices, causing a deviation in the flow field generated by the leading scales and preventing the formation of well-defined recirculation zones between the trailing scales. Although this affects drag reduction, recirculation zones remain present in front of and behind the scales, it still providing a slight acceleration effect, which helps maintain a low recirculation zone near the trailing edge of the blade.

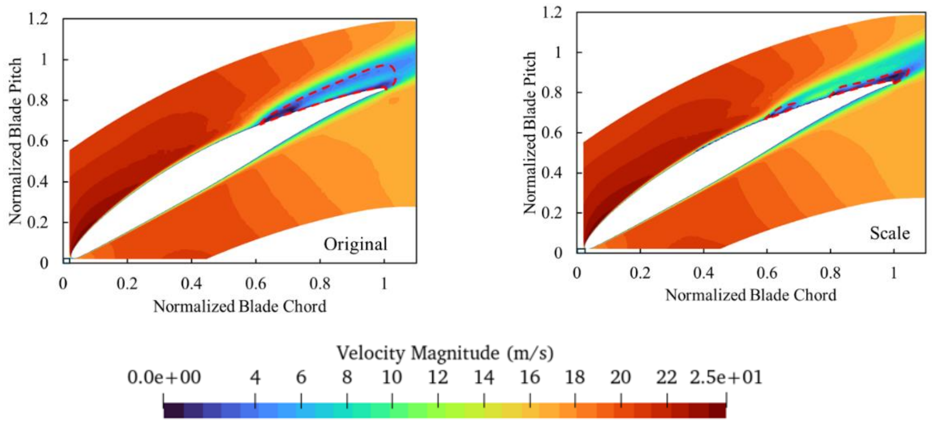


**Fig. 6 Comparison of velocity fields between traditional blade cascade (left) and bionic fish scale blade cascade (right) at z/h=0.044**

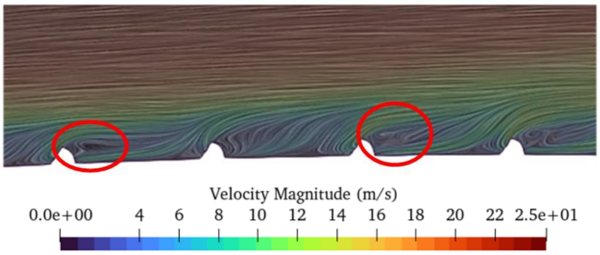


**Fig. 7 The velocity field streamline of the bionic fish scale blade at z/h=0.044**

To provide a more intuitive comparison of the secondary flow vortex structure strength and total pressure loss between the two cascades, Fig. 8 illustrates the findings. Compared to the traditional cascade, the concentrated shedding vortices in the biomimetic fish scale cascade are significantly reduced, leading to a decrease in total pressure loss. Additionally, the vortices generated by the fish scales rotate in the same clockwise direction as the channel vortex, increasing the intensity and size of the channel vortex. However, the flow field generated by the fish scales restricts the expansion of the channel vortex, preventing it from exceeding the vortex flow field produced by the fish scales. Moreover, the influence of the channel vortex confines the position and extent of the corner vortex, keeping it closer to the endwall surface.

The largest source of secondary flow losses is the concentrated shedding vortex. Therefore, an analysis of the area size and loss values associated with this vortex was conducted, as shown in Fig. 9. Compared to the traditional cascade, the total pressure loss region in the biomimetic fish scale cascade is significantly reduced. Additionally, near the mid-span of the blade, where the blade wake occurs, the spanwise influence of the concentrated shedding vortex in the biomimetic fish scale cascade is smaller. This provides a clearer understanding of the total pressure loss in the biomimetic fish scale cascade, demonstrating that the overall loss is reduced.

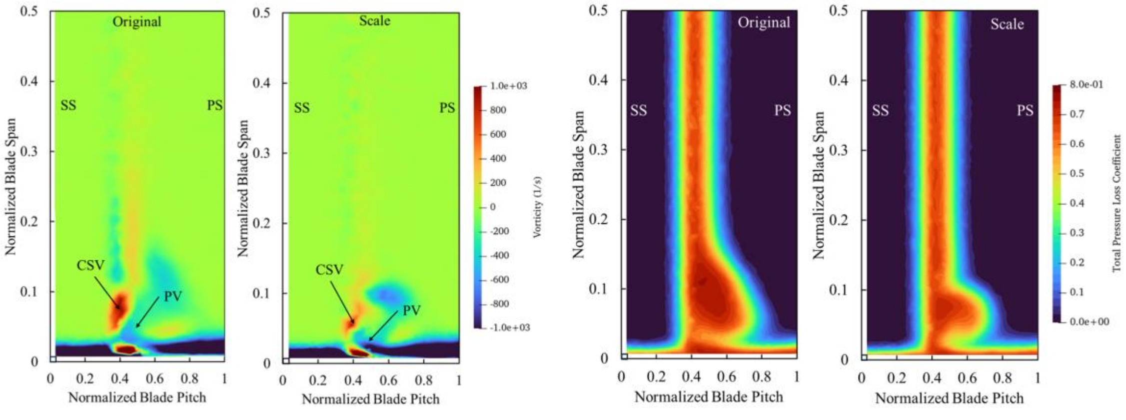


**Fig. 8 Comparison of streamwise vorticity(left) and total pressure loss(right) on the outlet measuring flat piece of traditional cascade and bionic fish scale cascade**

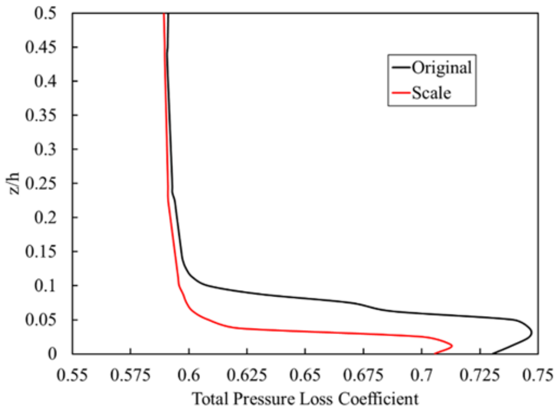


**Fig. 9 Distribution of total pressure loss at outlet measurement section**

## 4. Conclusion

In flat-plate flow fields, the regions between fish scales, particularly at the leading and trailing edges, create recirculation zones that are crucial for reducing viscous drag. For scales with a height of 0.4 mm, these zones are well-maintained, but increasing the height can diminish the effectiveness of these zones, leading to increased pressure drag and reduced drag reduction, potentially even having negative effects. When the spacing between scales increases from 3 mm to 6 mm, the recirculation zones are largely confined to the scale edges, reducing the drag reduction effect. Additionally, optimal drag reduction occurs at a scale height of 0.4 mm, with a spacing of 2 mm, under fixed parameters. The grass carp's scales, combining the benefits of whale fins and fish scales, show promise for application in compressor cascades.

In biomimetic cascades, fish scale structures effectively suppress the development of corner separation lines and reduce the impact of horseshoe vortices on secondary flow recirculation zones and subsequent concentrated shedding vortices, thus lowering secondary flow losses. However, the beneficial recirculation effects between scales are diminished in areas with larger curvature at the blade trailing edges due to shape and passage vortex influences. Despite this, the vortices generated by the scales continue to accelerate flow in the recirculation zones effectively, reducing the size and impact of concentrated shedding vortices. The results show that the application of biomimetic fish scale structures in compressor cascades significantly reduces secondary flow losses and total pressure loss compared to traditional designs, demonstrating their potential practical value.

## References


[1] Bhushan, B., Biomimetics: lessons from nature–an overview. Philosophical Transactions of the Royal Society A: Mathematical, Physical and Engineering Sciences, 2009. 367(1893): p. 1445-1486.

[2] Bushnell, D.M. and K. Moore, Drag reduction in nature. Annual review of fluid mechanics, 1991. 23(1): p. 65-79.

[3] Zhang, M., et al., A review on modeling of bionic flow control methods for large-scale wind turbine blades. Journal of Thermal Science, 2021. 30: p. 743-757.

[4] Cao, H., et al., Flow topology and noise modeling of trailing edge serrations. Applied Acoustics, 2020. 168: p. 107423.

[5] Liu, Z., et al., Drag Reduction Performance of Triangular (V-groove) Riblets with Different Adjacent Height Ratios. Journal of Applied Fluid Mechanics, 2023. 16(4): p. 671-684.

[6] Dong, J., et al., Flow control mechanism of compressor cascade: A new leading-edge tubercles profiling method based on sine and attenuation function. Physics of Fluids, 2023. 35(6).